SUPPLEMENTARY MATERIAL

Impact of canopy disturbances on climate sensitivity of old-growth beech (*Fagus sylvatica* L.) forests

Antonia Kölzer[1], Davide Frigo[2], Edurne Martinez del Castillo[1], Frederick Reinig[1], Jan Esper[1,3], Ingo Heinrich[4,5,6], Burkhard Neuwirth[7], Michele Baliva[8], Gianluca Piovesan[8], Emanuele Ziaco[1*]

[1]Department of Geography, Johannes Gutenberg University, Mainz, Germany

[2]Department of Land, Environment, Agriculture and Forestry, University of Padova, Legnaro, Italy

[3]Global Change Research Institute (CzechGlobe), Czech Academy of Sciences, Brno, Czech Republic

[4]Department of Natural Sciences, German Archeological Institute (DAI), Berlin, Germany

[5]Section for Climate Dynamics and Landscape Evolution, German Research Centre for Geosciences (GFZ), Potsdam, Germany

[6]Department of Geography, Humboldt-University Berlin, Germany

[7]DeLaWi Tree-Ring Analyses, Windeck, Germany

[8]DEB, Department of Ecological and Biological Sciences, University of Tuscia, Viterbo, Italy

*Email: eziaco@uni-mainz.de

Supplementary Methods

Boundary line development

To develop the regional boundary line, the percentage radial growth change (GC) and prior growth (PG) were calculated annually for all ring-width series, following the method of Nowacki and Abrams (1997). For each year GC was calculated as follows:

$$GC = \frac{M2 - M1}{M1} * 100$$

where M1 represents the average growth rate over the preceding 10 years, and M2 represents the average growth rate over the subsequent 10 years.

The boundary line was constructed by dividing PG values into 0.25 mm yr^{-1} classes for PG less than 1 mm and 0.5 mm yr^{-1} classes for PG values greater than 1 mm (Splechtna et al., 2005). The 0.25 mm yr^{-1} classes were used to refine the boundary line for low PG values (PG < 1 mm yr^{-1}), as these often exhibit the largest growth capacity pulses, which can significantly influence the boundary line's shape (Ziaco et al., 2012). Figure S6 illustrates the relationship between PG and GC across our three sites, highlighting distinct, site-specific distributions. For each PG class, the highest GC values were selected, specifically the top 5 for each 0.25 mm yr^{-1} class and the top 10 for each 0.5 mm yr^{-1} class. To quantify the boundary line, linear, power, logarithmic, and exponential curves were fitted to the averages of the top 10 and top 5 percent GC values for each class. The function achieving the highest R^2 value was then selected (Tab. 2; Black and Abrams, 2003). Additionally, we created a boundary line for the full distribution range of European beech, based on the extensive pan-European tree-ring network from Klesse et al. (2024), and compared the fit of already published boundary lines with our data. Figure S7 illustrates that the BL for the full distribution and previously published BLs tend to underestimate the release potential at our specific study sites. This comparison reinforces our decision to use site-specific boundary lines to accurately capture the natural forest dynamics and frequent canopy openings characteristic of these old-growth forests.

To identify disturbance-related growth pulses, each pair of PG and GC values was compared against the regional boundary line, which represents the maximum possible growth response for a given prior growth rate. For the goal of this study, we defined those growth pulses exceeding 40 % of the boundary line were classified as major releases, while those between 25 % and 39.9 % were classified as moderate releases. Growth pulses below 25 % of the boundary line were considered not associated with ecological (i.e. canopy) disturbances. Major and moderate growth releases were aggregated by 5-year intervals to emphasize long-term patterns of disturbance events. All the calculations were done in the R software environment (R Development Core Team, 2010) using the package TRADER (Altman et al., 2014).

Supplementary References

Black, B.A., Abrams, M.D., 2003. Use of Boundary-Line Growth Patterns as a Basis for Dendroecological Release Criteria. Ecol. App. 13, 1733–1749.

Klesse, S., Peters, R.L., Alfaro-Sánchez, R., Badeau, V., Baittinger, C., Battipaglia, G., Bert, D., Biondi, F., Bosela, M., Budeanu, M., Čada, V., Camarero, J.J., Cavin, L., Claessens, H., Cretan, A.-M., Čufar, K., de Luis, M., Dorado-Liñan, I., Dulamsuren, C., Espelta, J.M., Garamszegi, B., Grabner, M., Gričar, J., Hacket-Pain, A., Hansen, J.K., Hartl, C., Hevia, A., Hobi, M., Janda, P., Jump, A.S., Kašpar, J., Kazimirović, M., Keren, S., Kreyling, J., Land, A., Latte, N., Lebourgeois, F., Leuschner, C., Lévesque, M., Longares, L.A., Martinez del Castillo, E., Menzel, A., Merela, M., Mikoláš, M., Motta, R., Muffler, L., Neycken, A., Nola, P., Panayotov, M., Petritan, A.M., Petritan, I.C., Popa, I., Prislan, P., Levanič, T., Roibu, C.-C., Rubio-Cuadrado, Á., Sánchez-Salguero, R., Šamonil, P., Stajič, B., Svoboda, M., Tognetti, R., Toromani, E., Trotsiuk, V., van der Maaten, E., van der Maaten-Theunissen, M., Vannoppen, A., Vašíčková, I., von Arx, G., Wilmking, M., Weigel, R., Zlatanov, T., Zang, C., Buras, A., 2024. European Beech tree-ring dataset 1952-2020. https://doi.org/10.16904/ENVIDAT.547

Nowacki, G.J., Abrams, M.D., 1997. Radial-Growth Averaging Criteria for Reconstruction Disturbance Histories from Presettlement-Origin Oaks. Ecol. Monogr. 67, 225. https://doi.org/10.2307/2963514

Ziaco, E., Di Filippo, A., Alessandrini, A., Baliva, M., D'andrea, E., Piovesan, G., 2012. Old-growth attributes in a network of Apennines (Italy) beech forests: Disentangling the role of past human interferences and biogeoclimate. Plant Biosystems, 146, 153–166. https://doi.org/10.1080/11263504.2011.650729

Supplementary Figures

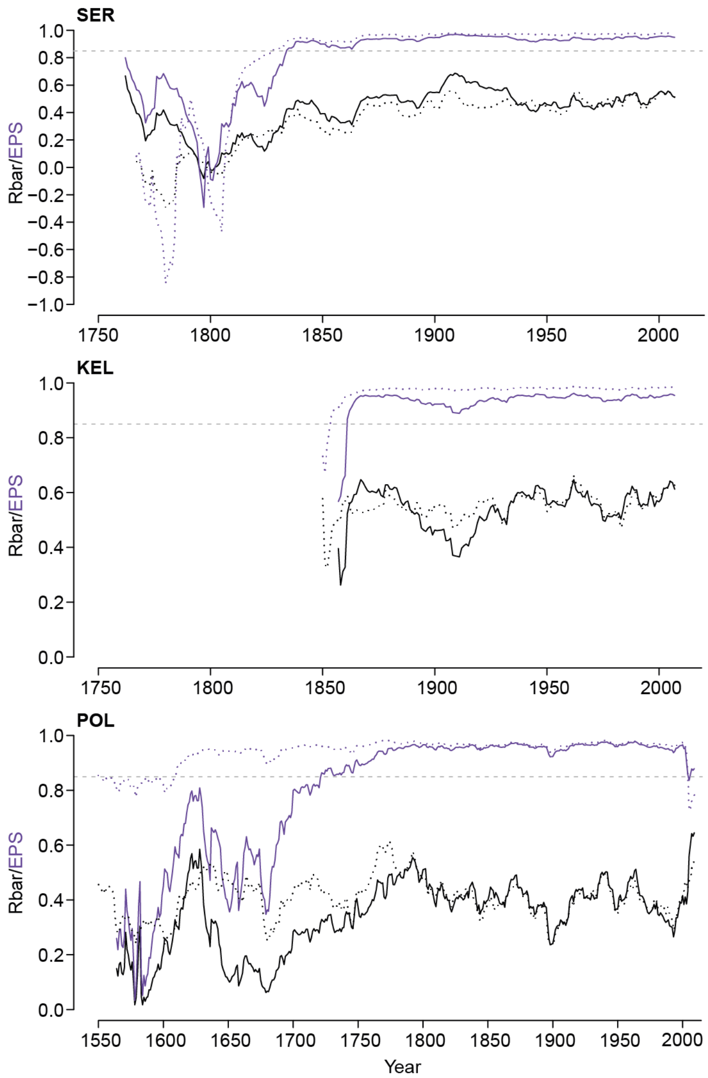

Figure S1: Running statistics. Temporal stability of Rbar (black) and EPS (purple) over a 30-year running window (moved by one year) for SER, KEL, and POL. Solid lines are undisturbed, and dotted lines are disturbed trees. The dashed grey line represents the 0.85 threshold for EPS.

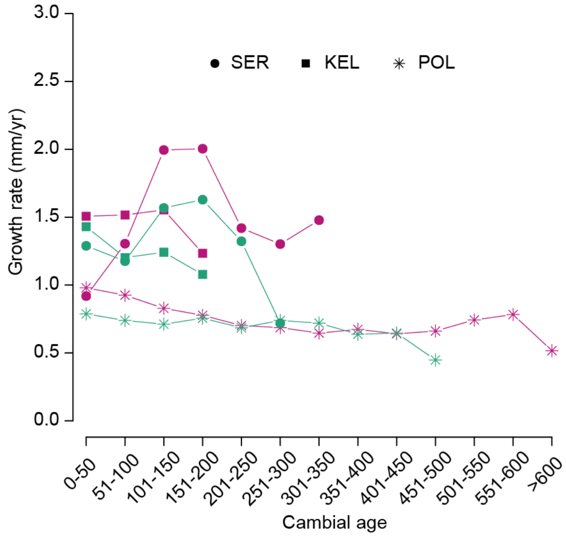

Figure S2: Mean annual growth rates for 50-year age classes for undisturbed (green) and disturbed (purple) trees for SER (dot), KEL (square), and POL (star).

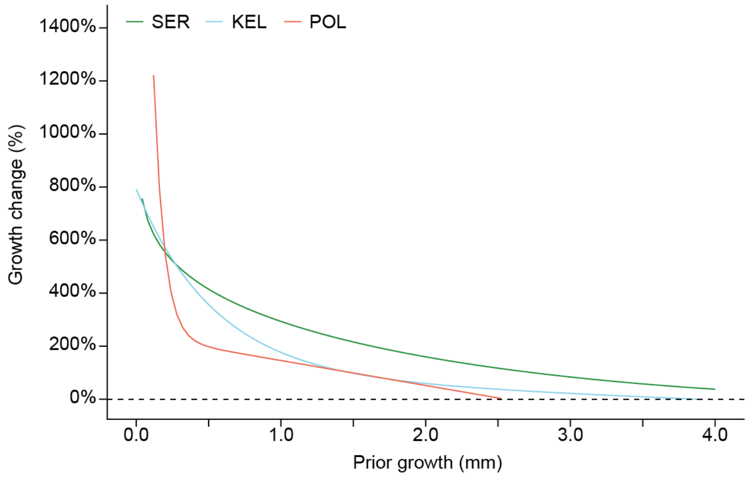

Figure S3: Comparison between the regional boundary lines developed for Serrahn (33.903 tree rings; green), Kellerwald (22.941 tree rings; light blue), and Pollinello (28.428 tree rings; red).

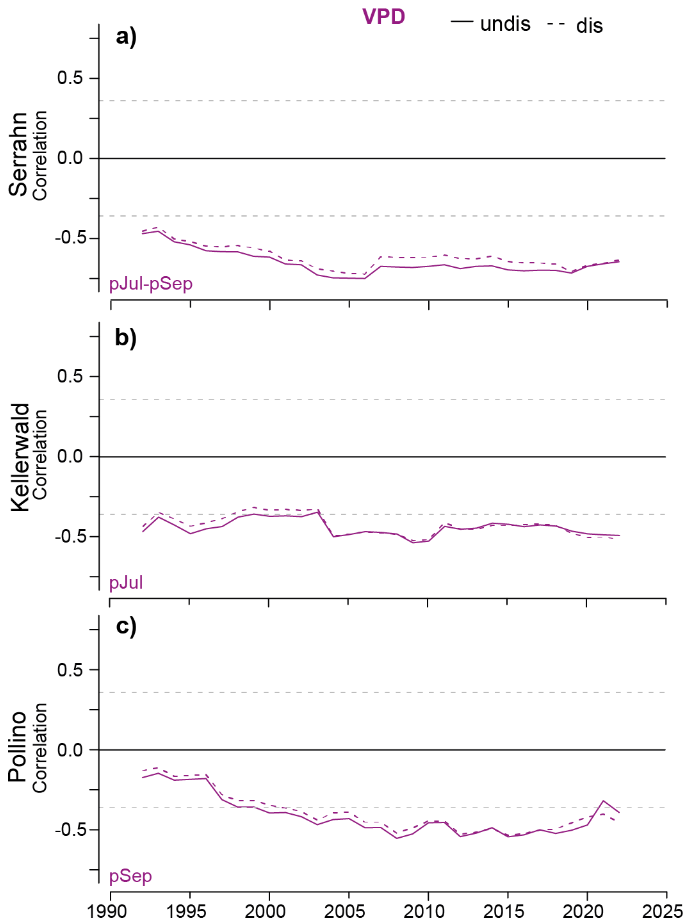

Fig. S4: 31-year moving correlations for the main VPD signal for undisturbed (solid) and disturbed (dashed) chronologies Serrahn (a), Kellerwald (b), and Pollinello (c) for the full period 1962-2022. Corresponding response periods when different are arranged as undisturbed/disturbed. Horizontal dashed lines indicate the statistically significant threshold of $p < 0.05$.

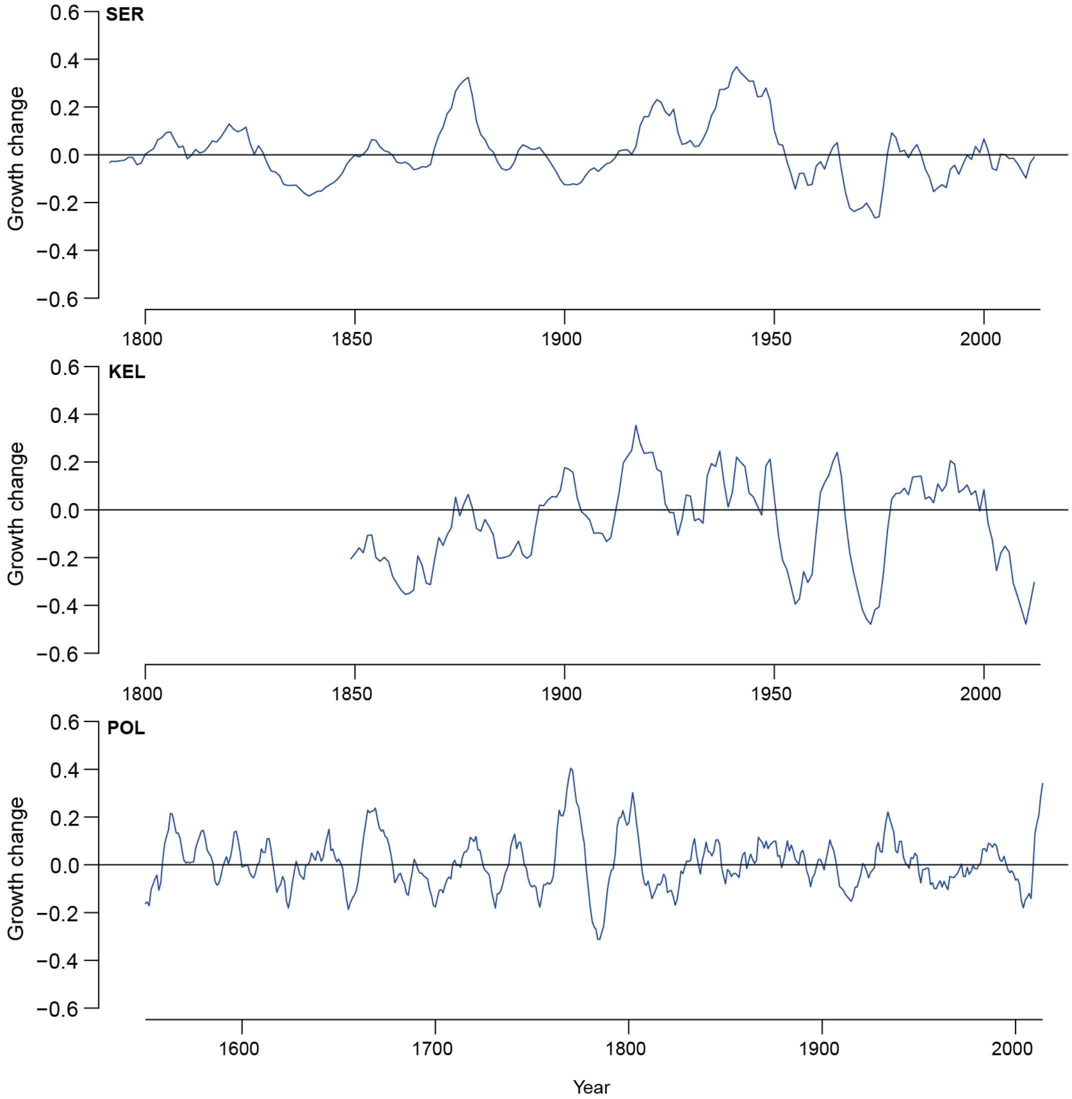

Fig. S5: Growth change chronologies for Serrahn (SER), Kellerwald (KEL), and Pollinello (POL)

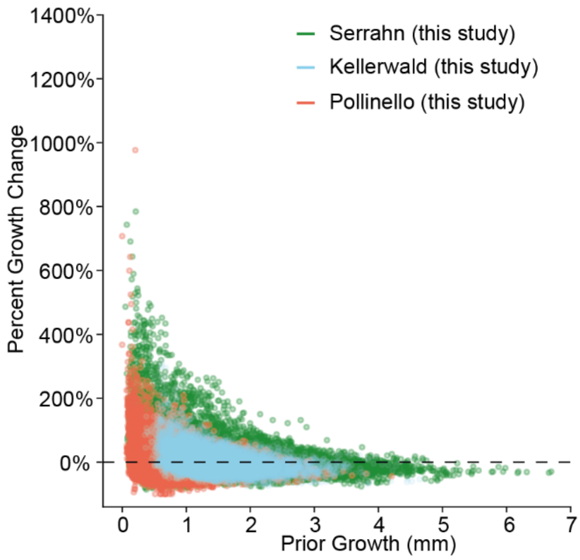

Fig. S6: Relationship between prior growth (PG) and percent growth change (GC) computed for the beech populations in Serrahn (green), Kellerwald (blue), and Pollino (red).

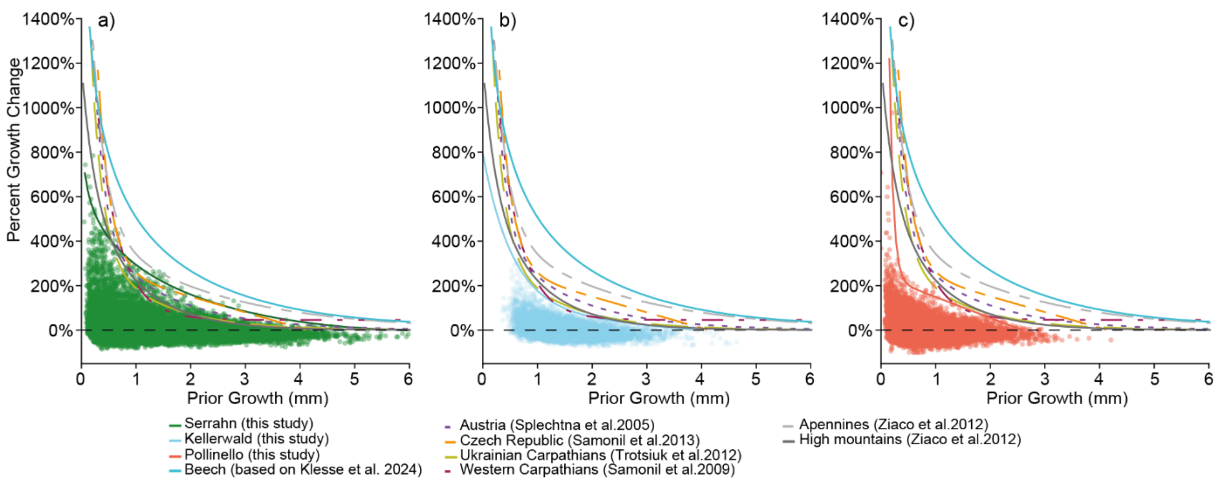

Fig. S7: Comparison of different regional boundary lines developed for *Fagus sylvatica* L. with the data for a) Serrahn, b) Kellerwald, and c) Pollino.

Supplementary Tables

Table S1: Statistical parameters of the boundary lines developed for the three study sites. For each site, the type of function, formula, and parameters used to calculate the boundary line are reported, describing the maximum potential growth change (GC) as a function of prior growth (PG).

Site	Function	Formula	Parameters				R^2
			a	***b***	***c***	***d***	
Serrahn	Log-linear	$GC = a + (b * GC) + (c * \ln(PG)) + (d * PG * \ln(PG))$	4.23	-1.29	-1.08	0.51	0.99
Kellerwald	Exponential-linear	$GC = a + (b * PG) + (c^{d*PG})$	0.86	-0.22	7.06	-1.83	0.99
Pollino	Exponential-linear	$GC = a + (b * PG) + (c^{d*PG})$	2.40	-0.94	52.78	-13.92	0.97

Table S2: Additional ITRDB-sites used for the development of the regional boundary lines.

	ITRDB sites	Cores (n)	Tree rings (n)
Serrahn	Germ217	48	6375
	Germ219	48	5841
	Germ221	46	5053
Kellerwald	Germ148	13	1850
	Germ149	15	2303
	Germ151	13	2319
	Germ152	16	3196

Table S3: Comparison of climate-growth correlation values for changing response windows. All pairings are non-significant, $p > 0.05$.

		Serrahn			***Kellerwald***			***Pollinello***		
		response window	1902-2022	1962-2022	response window	1902-2022	1962-2022	response window	1902-2022	1962-2022
undisturbed	Tmax	-	-	-	-	-	-	cApr	**-0.22**	-0.16
		-	-	-	-	-	-	pJun-pSep	-0.20	**-0.24**
	Ppt	pJun-pSep	**0.32**	0.31	pJul-pOct	**0.44**	0.55	-	-	-
		pJun-pOct	0.31	**0.31**	pJun-pOct	0.43	**0.52**	-	-	-
	SPEI	-	-	-	pJul-pSep	**0.40**	0.54	pJun-pAug	**0.32**	0.35
		-	-	-	pJun-pAug	0.37	**0.56**	pMay-pJul	0.25	**0.36**
	CC	pJun-pOct	**0.53**	0.53	-	-	-	-	-	-
		pJun-pAug	0.52	**0.54**	-	-	-	-	-	-
	DTR	pJun-pSep	**-0.52**	-0.52	-	-	-	-	-	-
		pJul-pSep	-0.50	**-0.53**	-	-	-	-	-	-

disturbed	Tmax	-	-	-	-	-	-	cApr	**-0.20**	-0.15
		-	-	-	-	-	-	pJun-pSep	-0.19	**-0.20**
	Ppt	cJan-cJun	**0.27**	0.27	pJul-pOct	**0.41**	0.38	-	-	-
		cApr-cSep	0.24	**0.30**	pJun-pOct	0.39	**0.50**	-	-	-
	SPEI	cApr-cJun	**0.36**	0.39	pJul-pSep	**0.37**	0.50	pJun-pAug	**0.32**	0.33
		pJul-pSep	0.35	**0.41**	pJun-pAug	0.32	**0.53**	pMay-pJul	0.26	**0.35**
	CC	pJun-pSep	**0.43**	0.46	-	-	-	-	-	-
		pJun-pOct	0.42	**0.46**	-	-	-	-	-	-
	DTR	-	-	-	-	-	-	-	-	-
		-	-	-	-	-	-	-	-	-
all	Tmax	-	-	-	-	-	-	cApr	**-0.22**	-0.17
		-	-	-	-	-	-	pJun-pSep	-0.19	**-0.23**
	Ppt	pJul-pSep	**0.29**	0.27	pJul-pOct	**0.42**	0.49	-	-	-
		cApr-cSep	0.23	**0.29**	pJun-pOct	0.40	**0.52**	-	-	-
	SPEI	-	-	-	pJul-pSep	**0.38**	0.52	pJun-pAug	**0.33**	0.35
		-	-	-	pJun-pAug	0.33	**0.54**	pMay-pJul	0.26	**0.36**
	CC	pJun-pSep	**0.46**	0.49	-	-	-	-	-	-
		pJun-pOct	0.46	**0.49**	-	-	-	-	-	-
	DTR	pJul-pSep	**-0.47**	-0.48	-	-	-	-	-	-
		pJun-pSep	-0.46	**-0.51**	-	-	-	-	-	-